resources

MDPI

Article

Flotation Recovery of Sphalerite in Sea Water: A Feasibility Study

Alexander A. Nikolaev

Department of Mineral Processing and Technogenic Raw Materials, National University of Science and Technology MISIS, 4 Leninsky Prospect, Moscow 119049, Russia; nikolaevopr@mail.ru

Abstract: Mining and mineral processing industry adversely affects ecosystems and communities in nearby areas, including high freshwater consumption and scarcity. That is why the emerging global trend is to use sea water in flotation to recover valuable minerals from finely disseminated base metals ores. Recent studies investigate sea water flotation of copper, molybdenum, nickel sulphides and pyrite, while flotation of sphalerite, the main valuable mineral for zinc production, remains uncovered. This paper examines the feasibility of sphalerite flotation by conventional collectors in artificial sea water using a bubble-particles technique and frothless flotation tests. Potassium isopropyl xanthate (PIPX) and sodium isopropyl dithiophosphate (SIDTP) were used as collectors, and copper sulphate was introduced as the activator, while zinc sulphate and sodium sulphide were used as depressants. We examined the most common size fractions of sphalerite: medium (−74 + 44 μm) and fines (−44 μm). The findings showed the feasibility of sphalerite flotation in artificial sea water. We also established correlations between the rate of bubble-particle attachment and the sphalerite flotation recovery resulting in the growth of flotation recovery with the increase of the bubble-particle attachment rate. The results can be used as guidelines in choosing flotation reagents for sphalerite flotation in sea water. Another practical application of the results is the potential for sustainable development of the industrial sector, ecosystems and societies due to the replacement of fresh water by sea water, although further technological and environmental studies are required.

Keywords: sea water flotation; sphalerite; thiol collectors; bubble-particles attachment; base metals ores processing; sustainability

Citation: Nikolaev, A.A. Flotation Recovery of Sphalerite in Sea Water: A Feasibility Study. *Resources* **2023**, *12*, 51. https://doi.org/10.3390/resources12040051

Academic Editors: Katharina Gugerell, Gregory Poelzer and Andreas Endl

Received: 30 January 2023
Revised: 24 March 2023
Accepted: 6 April 2023
Published: 12 April 2023

1. Introduction

The mining and mineral processing industry adversely affects ecosystems and communities in nearby areas [1–3]. The global increase in metals consumption with respect to resource depletion, a decrease in metal ores grade, and industrial waste treatment result in the growth of extraction and processing output of mineral raw materials [1,4,5].

Froth flotation is the most common method for beneficiation of low-grade ores [6–8] with high water consumption. Freshwater brings only 2.5% to the total water resources on Earth, while sea water incorporates the rest, 97.5% [9–11]. Traditionally, mineral processing plants use freshwater (lakes, rivers, and groundwater). However, due to freshwater scarcity, the sea and saline water are used alternatively [11–16]. In some regions, the mining and mineral processing sector significantly reduces the water availability of ecosystems and local communities because the consumption of water surpasses the carrying capacities [17].

Moreover, the policymakers and industrial sector need to implement a sustainable development approach for metals extraction and land use planning, including water resources [1,5,18,19]. Specifically, mineral processing plants are widely using sea water for the flotation of different types of raw mineral materials [11–13]. Figure 1 shows the length and altitude of pipelines and their total sum to supply sea water to mining operators worldwide.

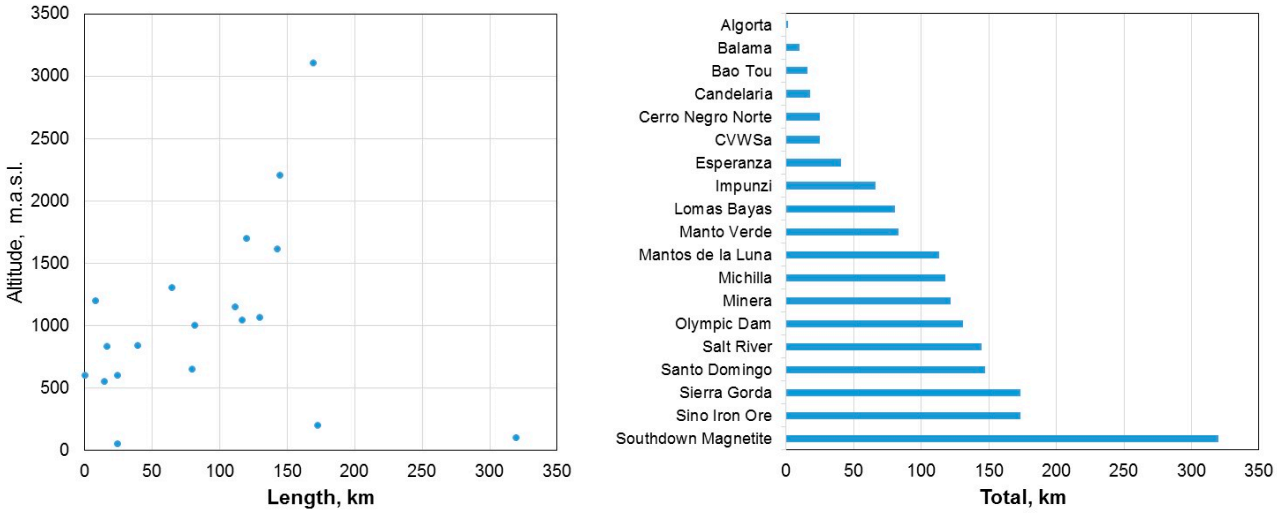

(**a**) (**b**)

Figure 1. The length and altitude of current pipelines (**a**) and their total sum (**b**) to supply sea water to mining operators worldwide(Data from [20]).

As can be seen, using sea water is feasible in the mining sector even if the sea water is supplied via hundreds of kilometres of pipelines to mining and mineral processing plants. Apart from the economic efficiency for the industry, using sea water instead of freshwater can safeguard the local ecosystems. However, further investigations of mineral flotation applications with respect to specific minerals are required.

The study [21] reported a depression effect of artificial sea water on the floatability of molybdenite and chalcopyrite in the absence of flotation reagents at pH > 9. The depression of chalcopyrite flotation in sea water is attributed to the effect of Ca^{2+}, Mg^{2+} and slime gangue minerals, which can be reduced by sodium silicate addition during collectorless flotation of chalcopyrite under alkaline conditions [22,23]. Moreover, oily collectors are required for differential flotation of molybdenite from chalcopyrite at alkaline pH. [21,24]. Apart from molybdenite, the sulphydryl collectors are used for the flotation of copper, nickel, zinc sulphide and pyrite [23,25,26]. The most commonly used collectors for the flotation of sulphide minerals are xanthates and dithiophosphates of alkaline metals [8,27]. However, to enhance sphalerite flotation, an activating reagent (copper sulphate) is introduced [7,28].

Furthermore, using small-scale techniques to analyse the feasibility of mineral flotation seems to be effective in reducing environmental impact and research and development costs. Moreover, the bubble-particle attachment phenomenon is widely considered a determining factor in flotation. Uddin et al. [29] used a pendant air bubble immersed in an agitated suspension and a digital camera to study the attachment of hydrophobic and non-hydrophobic fines. Later study [30] quantified a non-hydrophobic particle pickup correlated with the difference in zeta-potential with the bubbles. Our previous studies [31–36] examined the effects of collector and activator, their type and concentration, and hydrodynamic regimen on the attachment kinetics of air bubbles with sulphide minerals and toner particles in water using a pendant bubble technique and an image analysis.

Although the usage of sea water as a water resource for the mining and mineral processing industry is a reality, there are challenges [12]. Most studies investigate sea water flotation of copper, molybdenum, nickel sulphides and pyrite since the flotation of other base metals, such as sphalerite, which is the main valuable mineral for zinc production, is still uncovered. Moreover, high sea water salinity affects the surface properties of minerals, reagents and bubbles, resulting in insufficient metal recovery and grades of metal concentrates. In our opinion, using diluted sea water might improve those issues. This paper examines the feasibility of flotation recovery of sphalerite with sulphhydryl collectors

in artificial sea water using small-scale techniques to investigate the possible effects of flotation recovery of sphalerite from base metals ores in sea water.

2. Materials and Methods

2.1. Minerals and Reagents

A sample of lump sphalerite was crushed, dry ground and sieved to obtain size fractions −74 + 44 µm and −44 µm, and then sealed and stored separately to prevent air and water access.

Potassium isopropyl xanthate (PIPX) and sodium isopropyl dithiophosphate (SIDTP) were used as collectors, and copper sulphate was chosen as an activator reagent. Zinc sulphate and sodium sulphide were used as depressants of sphalerite with the addition of lime to adjust pH. Concentrations of solutions of reagents were 0.01% and 0.1%. Natural sea salt was dissolved in distilled water to obtain artificial sea water solutions with a salinity of 2 g/L and 8 g/L. Then each solution of flotation reagents was prepared using artificial sea water. The composition of sea salt: NaCl (81%), $MgCl_2$ (10.6%), $MgSO_4$ (4.4%), $CaSO_4$ (3.7%), and $CaCO_3$ (0.3%).

2.2. SEM Analysis

The sphalerite sample was analysed using a scanning electron microscope (SEM) VEGA3 (TESCAN, Brno, Czech Republic) operating at 20 kV with a LaB6 cathode and an energy-dispersive X-ray microanalysis system (Oxford Instruments Advanced AZtecEnergy, UK). We used backscattered electron and secondary electron imaging for the analysis. The statistical error of the detector for the determination of element concentrations using X-ray analysis was 0.2 wt%. Before SEM analysis, the sphalerite powder samples were placed on a sticky tape to achieve a monolayer, and then it was installed into a sample holder of the microscope. The chemical composition of the samples was analysed by collecting characteristic X-rays and using in-built software.

2.3. Technique for Studying Attachment Kinetics

Figure 2 shows an experimental apparatus for the investigation of the attachment kinetics of sphalerite particles to air bubbles [31–36].

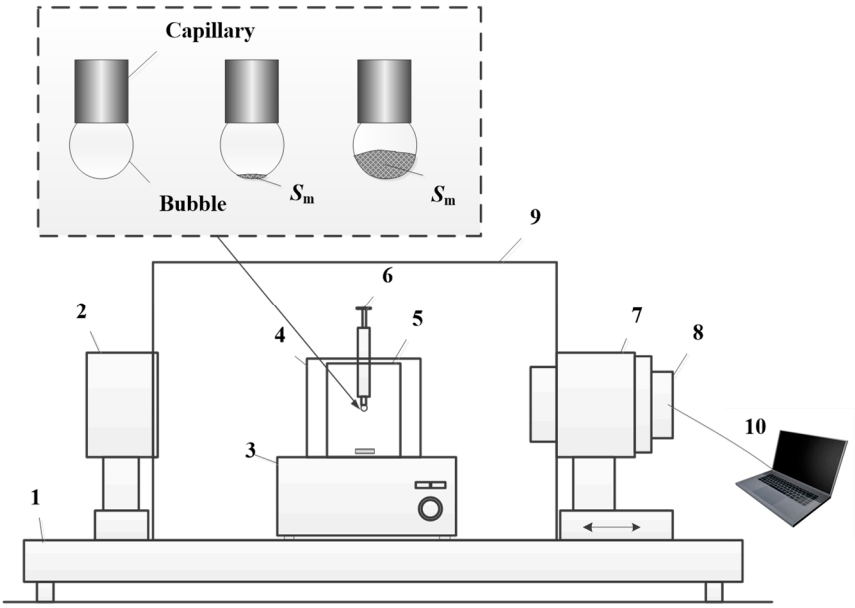

Figure 2. Experimental apparatus for attachment kinetic study: 1—vibration isolating platform; 2—illuminator and light filter; 3—magnetic stirrer; 4—cuvette; 5—glass beaker; 6—microsyringe; 7—optical system; 8—digital video camera; 9—cover box; 10—computer.

The apparatus consists of a plexiglass cuvette placed on a magnetic stirrer, a microsyringe with a capillary, an optical system, and a digital video camera. The items were installed on a vibration-isolating platform to prevent external effects. The digital camera was connected to the optical system of the microscope and plugged into a personal computer. The camera depicts the interaction of mineral particles with a gas bubble. The camera and the computer allow monitoring of bubble-particle attachment, capturing and saving images of the bubbles, and the bubbles covered with particles. The system was equipped with an illuminator, light filter and cover box to adjust the quality of images. The apparatus allows for capturing digital images of the bubbles covered with particles under stirring conditions of the suspension.

The sample of sphalerite (0.5 g) was placed into a glass beaker, and then a reagent solution (100 mL) was poured into it. The beaker was placed into the cuvette. Afterwards, a microsyringe was introduced into the suspension from the upper side along the vertical axis of the beaker, and an air bubble with an average diameter of 3 mm was formed at the end of a capillary. Further, the suspension was mixed for a fixed period of time, and then the magnetic stirrer was stopped. After the particles were settled, an image of the bubble with attached mineral particles was captured using the camera. Finally, a new air bubble was generated, and the procedure was repeated with other mixing times (15, 30, 60, 90, 120 and 180 s). The technique used for the attachment kinetic tests has been examined since 2012 and showed repeatability at 3–5 replicas; the relative standard deviation did not exceed 5.5%.

We processed images at constant resolution (640 × 480) using Adobe Photoshop CC 2019 software to estimate bubble loads with mineral particles. Specifically, we measured a 2D area in each image. First, the surface area of the bubble occupied by mineral particles was measured, and then the total area of the bubble and the particles on it was estimated. Finally, a relative surface coverage area (S) of the bubble with mineral particles was calculated [31,35]:

$$S = (S_m / S_{\sum}) \, 100\% \quad (1)$$

where S_m is the surface area occupied by mineral particles on the bubble; S_Σ is the total area of the bubble and the mineral load.

In our further studies, we examined attachment kinetic through a change of the relative surface area coverage of the air bubble with sphalerite particles for a specific period of time.

2.4. Frothless Flotation

Flotation tests were performed in a modified Hallimond tube, Figure 3.

A magnetic stirrer was used to suspend the particles in the medium. A sample of sphalerite (0.5–1 g) and a sea water solution of the collector were placed into the tube, conditioned and then the sphalerite sample was floated. Air was used as a gas phase at a constant flow rate of 40 cm^3/min. The flotation tests were conducted for 3 min. Floated and non-floated products were dried and weighed. Flotation recovery of sphalerite into the floated product was calculated:

$$\varepsilon = m_f \, 100\% / (m_f + m_{n.f}) \quad (2)$$

where m_f and $m_{n.f}$ are the masses of floated and non-floated products. We used three replica tests; the relative standard deviation did not exceed 5%.

Before each test with an activator and depressant, the mineral was conditioned for 3 min in a 100 mL glass beaker of preset salinity. We used the natural pH of solutions for the flotation tests with sphalerite activated by copper sulphate and pH 9 and 10 for studies with depressants. Then, a liquid phase was poured off, and sphalerite was transferred into the flotation tube with the addition of a collector solution.

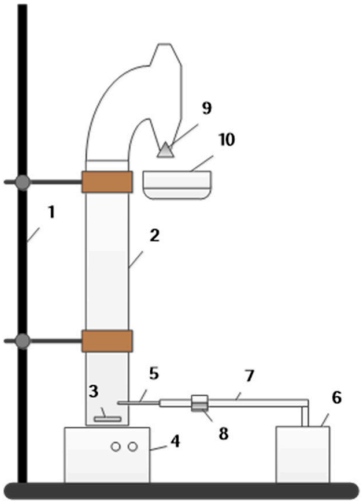

Figure 3. Sketch of a frothless flotation apparatus: 1—support stand; 2—bottom part of the tube; 3, 4—magnetic stirrer; 5—capillary tube; 6—air compressor; 7—flexible tubing; 8—valve; 9—stopper; 10—a vessel for collection of the floated product.

3. Results and Discussion

3.1. Sphalerite Sample Characterization

Figure 4 shows SEM images of sphalerite samples used in the study.

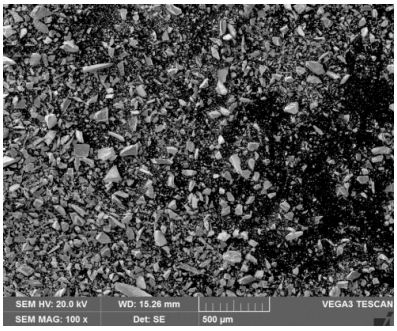

(**a**)

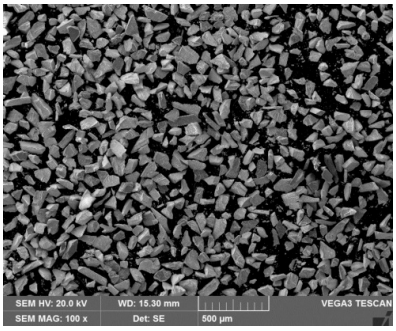

(**b**)

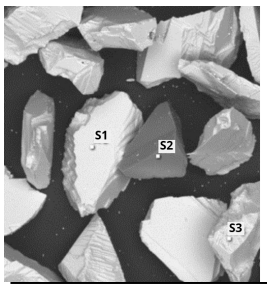

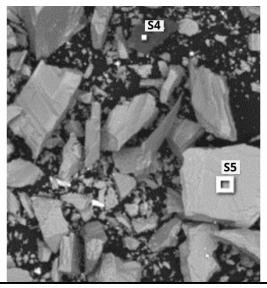

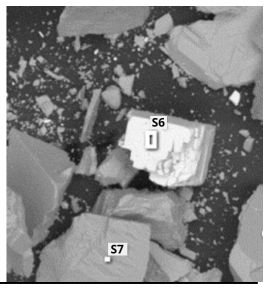

Spectrum Label	O	Si	S	Fe	Zn	Pb
S1			31.36	3.92	64.72	
S2	57.3	42.7				
S3			27.26	4.14	68.6	
S4	54.85	45.15				
S5			33.81	3.79	62.4	
S6			13.36			86.64
S7			37.84	6.26	55.91	

(**c**)

Figure 4. SEM images of sphalerite samples sized −44 µm (**a**) and −74 + 44 µm (**b**) and sample characterisation (**c**).

For the slimes (−44 µm) a significant number of finely dispersed sphalerite particles were observed. Moreover, SEM confirmed low iron content in sphalerite: 3.92–6.26% Fe, 55.91–68.6% Zn and 27.26–37.84% S. A few particles of galena were also detected in the samples.

The mineral composition of the bulk sample is summarised in Table 1.

Table 1. Mineral composition of the sample.

Mineral	Formula	Content %
Sphalerite	ZnS	95.72
Galena	PbS	3.43
Quartz	SiO_2	0.85
Total	-	100

3.2. Non-Activated Sphalerite Particles

Figure 5 shows the kinetics of a relative surface coverage area of air bubbles by non-activated sphalerite particles in sea water solutions of SIDTP and PIPX.

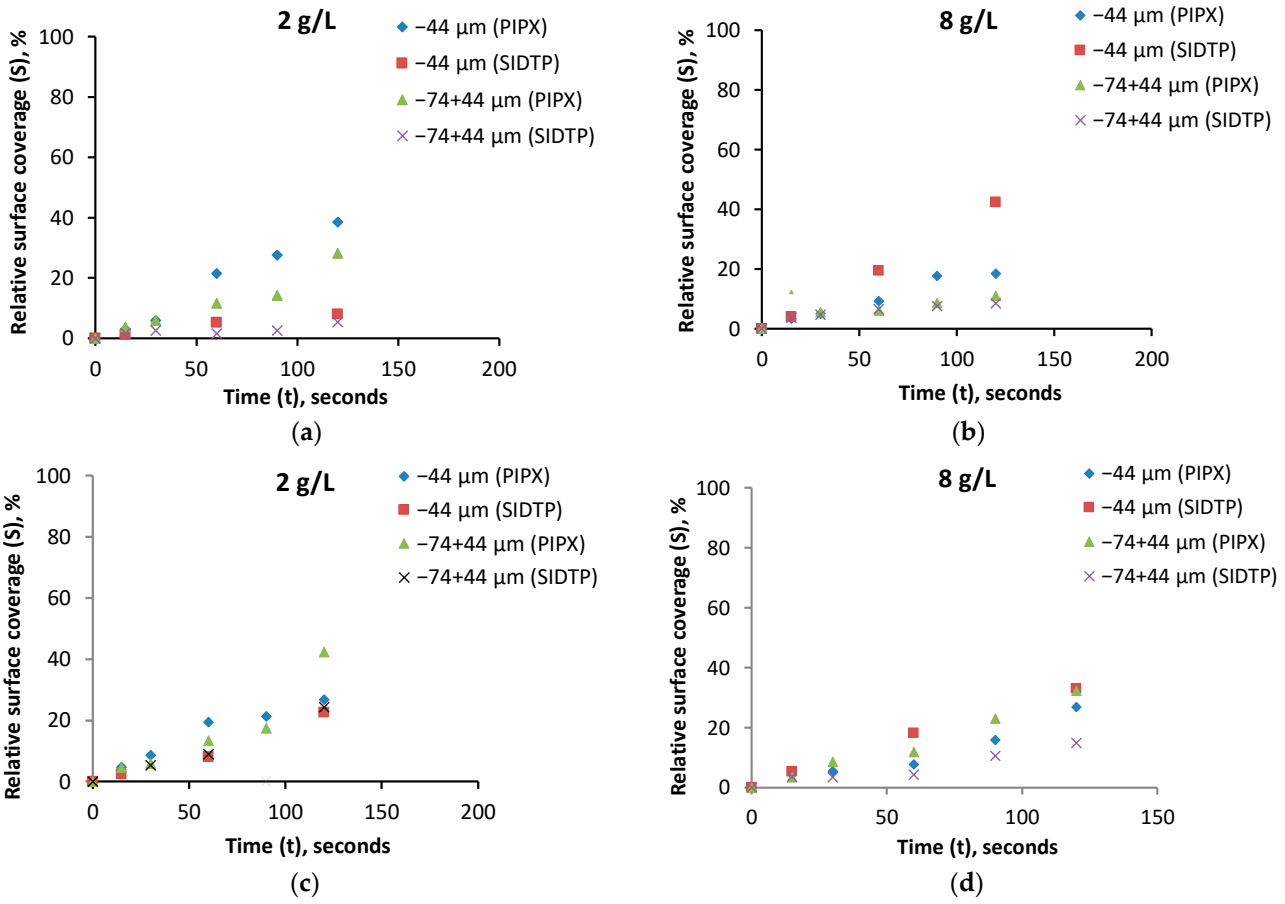

Figure 5. Kinetics of the surface coverage area of air bubbles by non-activated sphalerite particles in sea water solutions of collectors. The concentrations of the collectors are 0.01% (**a**,**b**) and 0.1% (**c**,**d**).

The relative surface coverage of the bubbles with non-activated sphalerite particles increased gradually with conditioning time. Within 15–30 s, the surface areas of the bubbles for both collectors were similar. Initially, at low concentrations of collectors (0.01%), the size of particles and nature of collectors insignificantly affected attachment kinetics (see Figure 5a,b). The differences appeared at conditioning times of $t \geq 60$ s. At water salinity of 2 g/L and the collector concentration of 0.01%, the surface coverage of the bubbles

increased in the following order: −74 + 44 µm (SIDTP), −44 µm (SIDTP), −74 + 44 µm (PIPX), −44 µm (PIPX), indicating the strong collector performs better than the weak one. Moreover, we can observe that the slimes are more readily attached to the bubbles than −74 + 44 µm sphalerite. Although at the salinity of 8 g/L, the slimes performed better than the sphalerite fractions of −74 + 44 µm, the effect of SIDTP on the surface coverage of the bubbles with the slimes was significantly higher than PIPX. Moreover, we observed similar trends in surface coverage of the bubbles with −74 + 44 µm fractions for both collectors at the salinity of 8 g/L. In general, at collectors' concentration of 0.01%, PIPX promoted attachment of −44 µm sphalerite particles to air bubbles in the sea water with a salinity of 2 g/L, whereas SIDTP performed better at the salinity of 8 g/L.

Increasing the collectors' concentration to 0.1% converged the data in the graphs (see Figure 5c,d), maintaining the tendency of increasing the bubble surface coverage over increasing the stirring time. The attachment kinetics of the bubbles with non-activated sphalerite particles for both −74 + 44 µm and −44 µm fractions showed a certain degree of linearity, meaning the surface coverage change was stable during the observed stirring time.

Although the attachment of the air bubbles with non-activated sphalerite particles in sea water solutions was investigated, for practical purposes, we also focus on the effect of copper sulphate on the attachment kinetics and flotation of sphalerite in saline water as the copper sulphate is widely used as the sphalerite flotation recovery promoter [7]. Further studies examine the attachment kinetics of the air bubbles with activated sphalerite particles in the sea water solutions.

3.3. Activated Sphalerite Particles

Figure 6 shows photographs of bubbles covered by activated sphalerite particles in sea water solutions of PIPX at different conditioning times. The concentrations of solutions of PIPX and $CuSO_4$ are 0.1%.

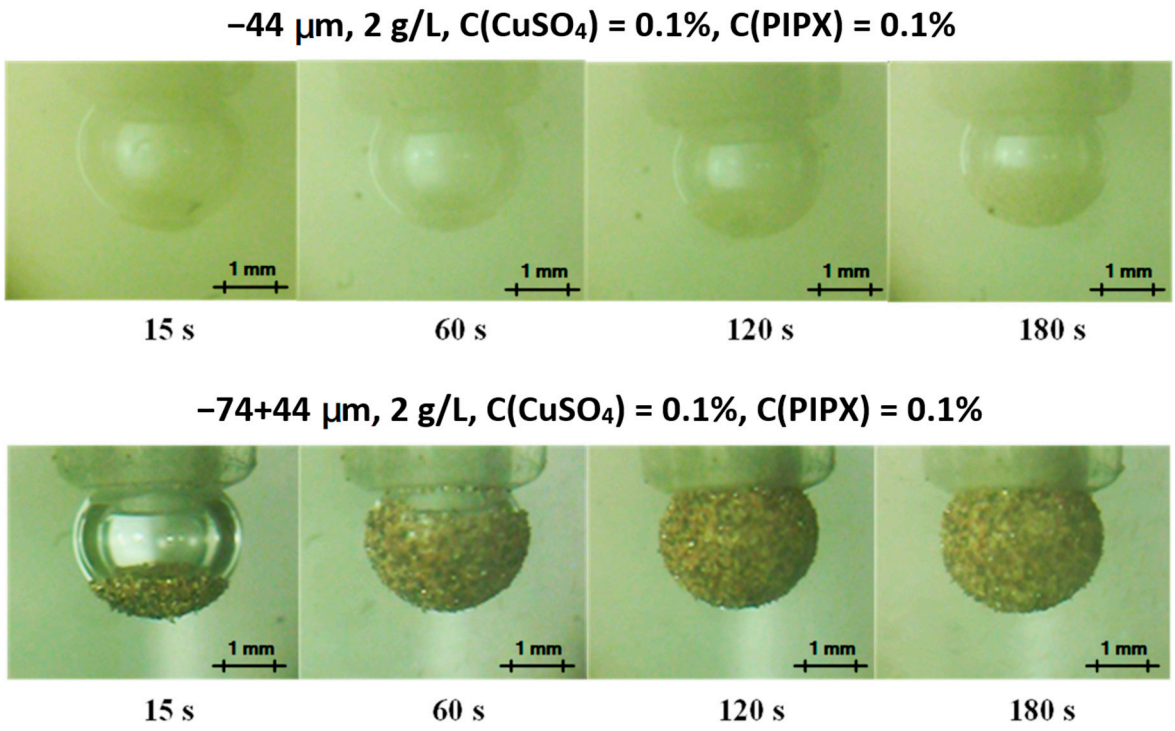

Figure 6. Microphotographs of activated sphalerite particles attached to air bubbles in sea water solutions of PIPX at different conditioning times.

The microphotographs show different effects of PIPX on the attachment kinetics of slimes and medium-sized sphalerite. For the activated sphalerite fractions of −74 + 44 µm,

the surface coverage of the bubbles increased sharply with conditioning time, and the bubbles were almost completely covered by particles at 60 s. Significant surface coverage of the bubbles by flotation size fractions of sphalerite at initial conditioning times can be attributed to the activation effect of copper sulphate on sphalerite (see Figure 6). In contrast, the slimes exhibited a gradually slower growth of the surface coverage than the sphalerite fraction of −74 + 44 µm. The most probable reasons for the lower surface coverage of the bubbles with the slimes can be explained by their high surface area, requiring more reagents dosages, or the surface chemistry, since the hydrodynamic mode in the cell was rather turbulent to allow bubble-particles collision [37]. The minor effect of copper sulphate on the surface coverage of the bubbles by slimes might indicate their lower floatability during flotation. We observed a similar effect during frothless flotation tests described in Section 3.4.

Figure 7 shows the bubble-particles attachment kinetics for the sphalerite particles activated by copper sulphate in sea water solutions of PIPX and SIDTP.

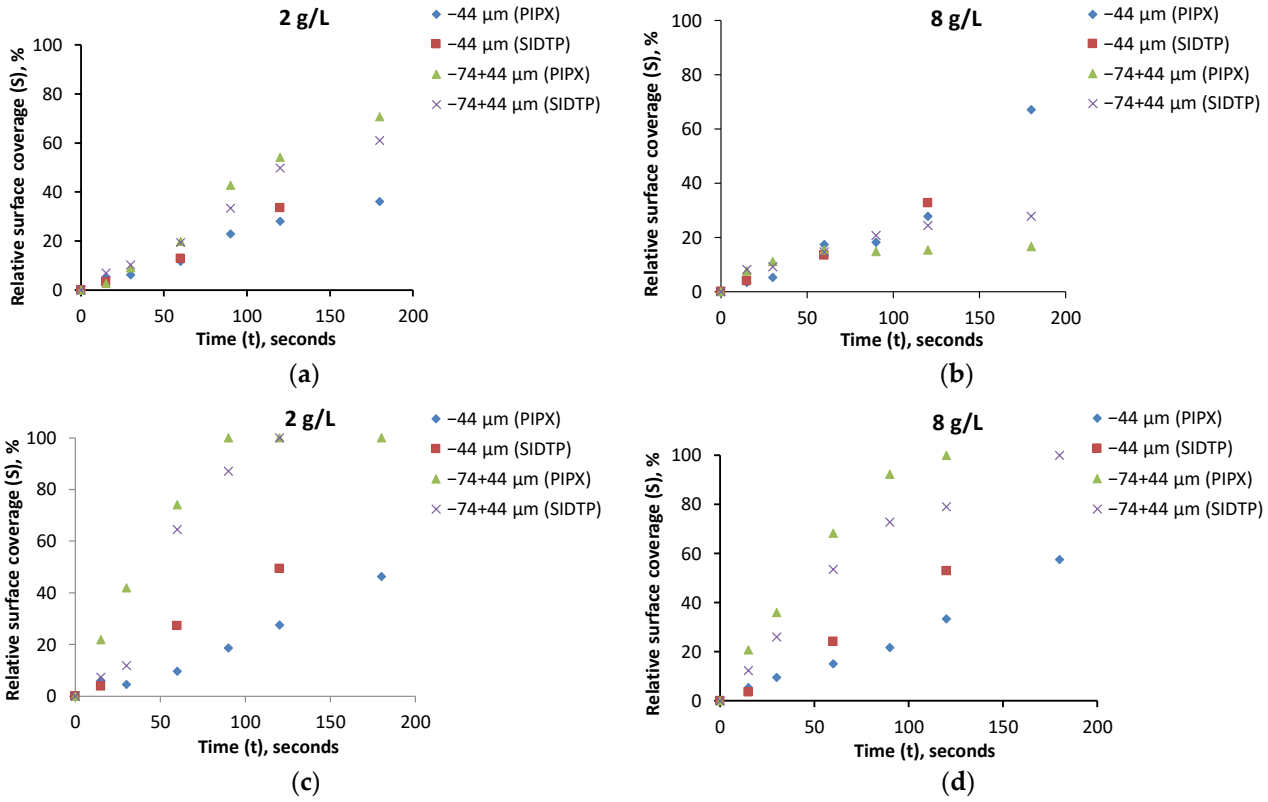

Figure 7. Kinetics of the surface coverage area of air bubbles by activated sphalerite particles in sea water solutions of collectors. The concentrations of the collectors and activator are 0.01% (**a**,**b**) and 0.1% (**c**,**d**).

We observed a higher surface coverage area for the sphalerite fractions of −74 + 44 µm than for the slimes. Specifically, high concentrations (0.1%) of CuSO4 and collectors' solutions significantly increased the surface coverage of the bubbles with −74 + 44 µm sphalerite particles. At the salinity of 2 g/L, the surface coverage increased sharply from 7.2% to 100% (SIDTP) and from 21.5% to 100% (PIPX) with the increase of conditioning time from 15 s to 120 s. Moreover, a strong collector (PIPX) demonstrated higher surface coverage of the bubbles by −74 + 44 µm sphalerite particles than a weak one (SIDTP) from the beginning of conditioning time until 90 s. Similarities were observed at the salinity of 8 g/L, increasing the conditioning time from 15 s to 120 s resulted in a growth of the relative surface coverage of the bubbles by −74 + 44 µm particles from 12.8% to 79.1% (SIDTP) and from 20.8% to 100% (PIPX). More time is required for SIDTP (180 s) to achieve 100% surface

coverage. Therefore, in sea water solutions with a salinity of 8 g/L, PIPX performed better than SIDTP with respect to the attachment kinetic of sphalerite particles of −74 + 44 μm. Moreover, we observed significantly higher surface coverage of the bubbles with activated sphalerite particles than with non-activated ones.

For the slimes, the effect of sphalerite activation with copper sulphate was lower than for the medium-sized fraction meaning the larger surface area of the slimes requires higher dosages of copper sulphate and collectors [38]. At the salinity of 2 g/L, increasing the conditioning time from 15 s to 120 s resulted in a growth of the surface coverage of the bubbles from 7.2% to 49.2% (SIDTP) and from 5.8% to 27.4% (PIPX), whereas at the salinity of 8 g/L, the surface coverage increased from 3.5% to 52.9% and from 5.4% to 33.4% respectively. To sum up, for the activated sphalerite particles of −44 μm, SIDTP performed better than PIPX.

We also estimated the bubble-particle attachment rates as the surface coverage change for the time of attachment. The kinetic attachment models for −74 + 44 μm sphalerite particles under conditions of $C(CuSO_4)$ = C(SIDTP) = C(PIPX) = 0.1%, where C is the concentration of reagent, were better fitted by the first order equation with the coefficient of determination R^2 = 0.95–1:

$$\ln(1/(1 - S)) = kt \quad (3)$$

where k = 0.0143–0.031 s^{-1} is the rate of bubble-particles attachment kinetics.

However, for the activated slimes, a linear model of bubble-particle attachment was best suited:

$$S = kt \quad (4)$$

where k is the rate of bubble-particles attachment kinetics, s^{-1}.

Differences in fitting Equations (3) and (4) indicate dissimilarities in bubble-particle attachment kinetics depending on particle size.

A linear model of the kinetics was also observed during the attachment of non-activated sphalerite particles to air bubbles for both PIPX and SIDTP solutions at low (0.01%) and high (0.1%) concentrations of the collectors.

Figure 8 shows fitting data for the attachment kinetics of the activated sphalerite slimes.

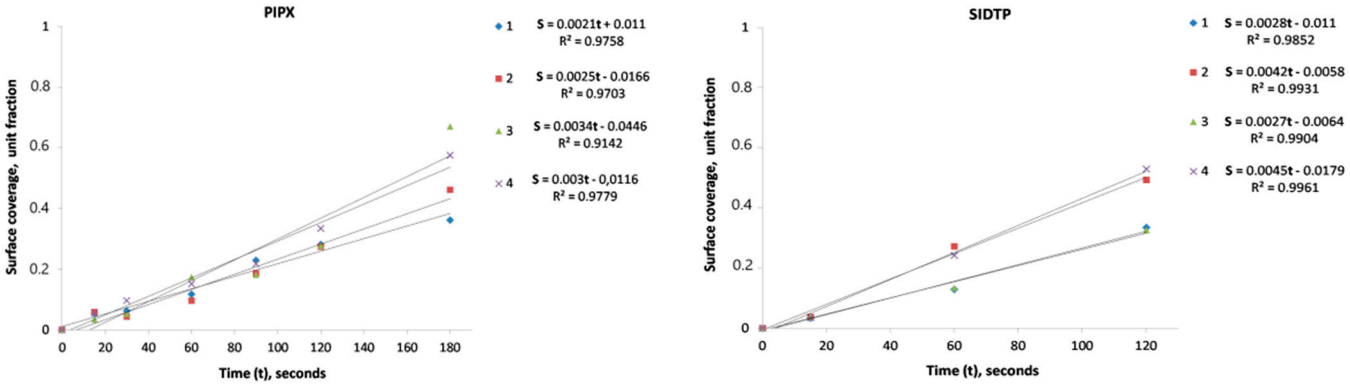

(**a**) (**b**)

Figure 8. Fitting data for the attachment kinetics of the activated sphalerite slimes: 1–2 g/L and C(collector) = 0.01%; 2–2 g/L and C(collector) = 0.1%; 3–8 g/L and C(collector) = 0.01%; 4–8 g/L and C(collector) = 0.1%. (**a**) PIPX; (**b**) SIDTP.

The effect of collector concentration on the rate of bubble-particle attachment kinetics was more pronounced for SIDTP than for PIPX. Specifically, at the salinity of 2 g/L, increasing the collector concentration resulted in the growth of k from 2.8 × 10^{-3} s^{-1} to 4.2 × 10^{-3} s^{-1} for SIDTP and from 2.1 × 10^{-3} s^{-1} to 2.5 × 10^{-3} s^{-1} for PIPX. Apparently, using PIPX requires less dosage than SIDTP to achieve similar surface coverage of the bubbles.

Figure 9 demonstrates photographs of copper-activated sphalerite particles attached to air bubbles in sea water solutions of PIPX and SIDTP at a constant conditioning time of 120 s.

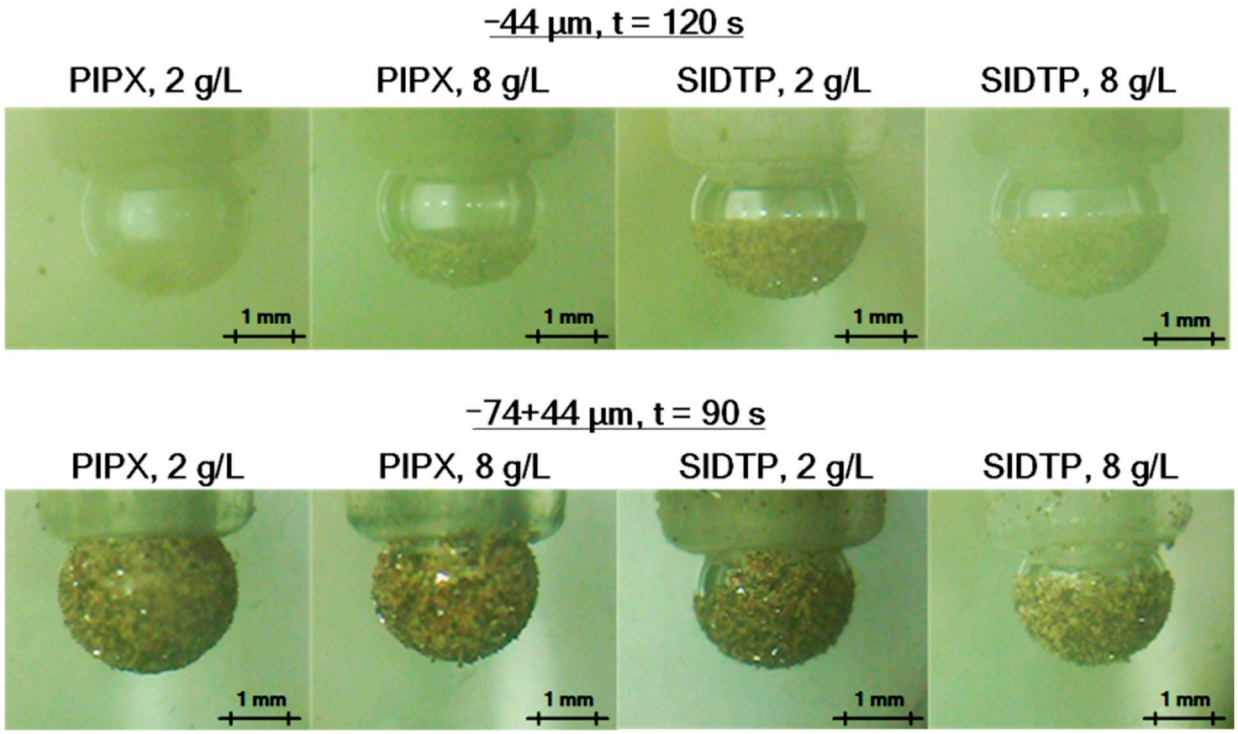

Figure 9. Attachment of copper-activated sphalerite particles onto air bubbles in sea water solutions of the collectors at constant conditioning time: C(PIPX) = C(SIDTP) = C($CuSO_4$) = 0.1%.

The observations indicate differences in the performance of the collectors between slimes and medium-sized fractions of activated sphalerite. For both collectors, the sphalerite fractions of −74 + 44 µm exhibited higher interactions with air bubbles and readily covered their surfaces than for −44 µm fractions. Although the slimes exhibited lower surface coverage of the bubbles, SIDTP performed better than PIPX.

The copper cations are commonly used to activate sphalerite flotation because of ion exchange on the sphalerite surface [39]:

$$ZnS_{(s)} + Cu^{2+} = CuS_{(s)} + Zn^{2+} \quad (5)$$

Moreover, if Pb^{2+} ions exist in the suspension, oxidised galena as a source of lead cations, they can activate the sphalerite flotation in a similar way:

$$ZnS_{(s)} + Pb^{2+} = PbS_{(s)} + Zn^{2+} \quad (6)$$

For the hydrated sphalerite surface, another reaction occurs [40]:

$$ZnS/ZnOH + PbOH^{+} = ZnS/Zn\text{-}O\text{-}Pb^{+} + OH^{-} \quad (7)$$

The observed sphalerite activation by metallic ions is typically considered a result of the increased pulp conductivity followed by collector adsorption, although lead cations have a smaller effect on the sphalerite flotation than copper ones [40,41].

Furthermore, the sulphides obtain a certain degree of hydrophobicity, and sea water ions compress the electrical double layer reducing the bubble-particle energy barrier and enhancing bubble-particles attachment [40,42]. Moreover, Jeldres et al. underline that the high electrolyte content of sea water can compress the electrical double layer between particles

and the bubbles. The authors conclude the attractive non-DLVO (Derjaguin-Landau-Verwey-Overbeek) and van der Waals forces are superior to repulsive ones enhancing bubble-particle attachment even for particles with low hydrophobicity [43].

Similarly, Peng et al. explained improved flotation of pentlandite in bore water because the addition of bore water compressed the electrical double layer of the particles reducing the magnitude of the zeta potential of pentlandite [44].

Also, Klassen and Mokrousov interpreted bubble–particle attachment in saline water because of reduced surface hydration of the particles in the inorganic electrolytes destabilising the hydrated layers surrounding particles [42].

The sea water contains Ca^{2+}, and hence, the hydrolysed ion species of Ca^{2+}, in addition to a high concentration of Cu^{2+}, can depress the sphalerite flotation lowering the surface coverage of the air bubbles with sphalerite fines [40]. Apparently, the depression effect is more pronounced for fines because of their high surface activity. Moreover, the surface interactions of sphalerite in sea water may result in decreasing the contact angle of the sphalerite surface treated with xanthates or dithiophosphates collectors, hence, reducing bubble-particle attachment and flotation [45].

Wang et al. explained the inhibition effect of high ion concentration on the potassium amyl xanthate adsorption on sphalerite in saline water by competitive adsorption [46]. Moreover, in saline water, the xanthate decomposition may take place at the sphalerite surface resulting in the adsorption of decomposition products on the particles. However, depending on flotation conditions, high salinity may have a beneficial impact on mineral flotation because of the electrical double-layer compression at the mineral-water interface. The reduced bubble-particle attachment of xanthate-treated sphalerite in saline water due to the negative zeta potential of sphalerite particles and bubbles can be improved by the bridging effect of Ca^{2+} and Mg^{2+} ions [46].

Hirajima et al. investigated the effect of Ca^{2+} and Mg^{2+} ions contained in sea water on the flotation recovery of chalcopyrite. The authors explained the depressed effect of $MgCl_2$ and $CaCl_2$ on chalcopyrite via the adsorption of hydrophilic complexes on the chalcopyrite surface, reducing the surface hydrophobicity. Moreover, the zeta potential measurements of chalcopyrite in Ca^{2+} and Mg^{2+} solutions showed the adsorption of precipitates onto the mineral surface [24]. Hence, the insufficient surface coverage of the bubbles with activated sphalerite particles of −44 µm in sea water can be partially attributed to the similar effect of Ca^{2+} and Mg^{2+} ions on the sphalerite surface.

To sum up, SIDTP improved the attachment of the slimes, while PIPX significantly increased the surface coverage of the bubbles by a medium-sized fraction of sphalerite, indicating −74 + 44 µm sphalerite can be better floated than the slimes. Our findings are in line with Wang et al. [39], who investigated bubble-particle attachments of another essential sulphide mineral, chalcopyrite, using thiol collectors, underlining the importance of attachment kinetics in collectors' performance assessment.

In the next section, we examined a frothless flotation of sphalerite in sea water solutions.

3.4. Frothless Flotation of Sphalerite

To demonstrate the effect of bubble-particle attachment rate on the flotation recovery and rate of different size fractions of sphalerite, we investigated sphalerite flotation under activation and depression conditions. Figure 10 shows the effect of the copper sulphate concentration on the flotation recovery and rate of attachment of the bubbles with sphalerite particles using PIPX at a water salinity of 2 g/L.

Increasing the concentration of copper sulphate from 0.01% to 0.1% resulted in the significant growth of flotation recovery of sphalerite (−74 + 44 µm) from 55% to 82% ($\Delta\varepsilon$ = 27%), whereas for the slimes, we observed its insignificant increase from 28% to 30%. The effect of copper sulphate concentration on the flotation rate (k_f) of sphalerite particles showed a similar trend. The flotation rate was calculated as a ratio of the flotation recovery of sphalerite to the time required for its flotation. Increasing the copper sulphate concentration increased the flotation rate of medium-sized sphalerite from 0.183 min^{-1}

to 0.273 min^{-1} and insignificantly affected the flotation rate of the slimes, demonstrating growth from 0.093 min^{-1} to 0.1 min^{-1}. In general, the flotation rate of −74 + 44 µm fraction of activated sphalerite was 2.0–2.7 times more than the −44 µm fraction.

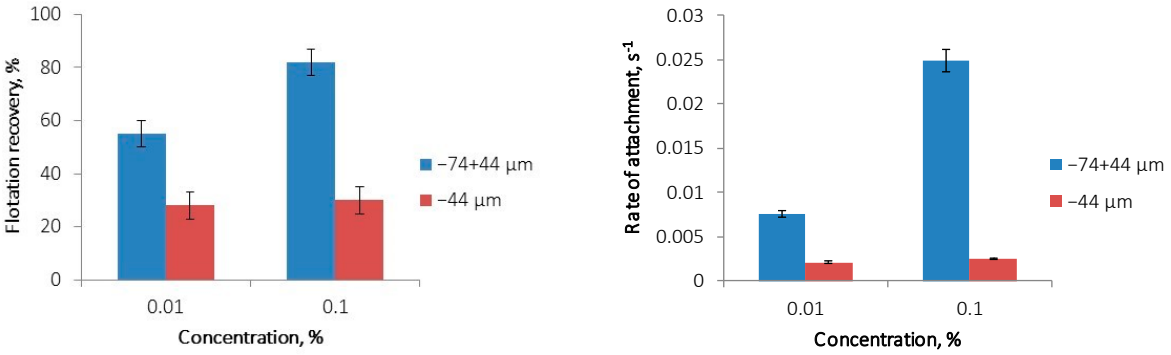

(**a**) (**b**)

Figure 10. Effect of the copper sulphate concentration on the flotation recovery (**a**) and rate of attachment (**b**) of the bubbles with sphalerite particles using PIPX at water salinity of 2 g/L.

Figure 11 demonstrates fitting experimental data for the effect of the rate of bubble-particle attachment on the flotation recovery, flotation rate, and surface coverage of the bubbles with sphalerite particles using PIPX at a water salinity of 2 g/L. Moreover, the effect of the surface coverage on sphalerite flotation recovery is shown. The fitting models were chosen based on the coefficient of determination (R^2) using MS Excel. A high R^2 value indicates that the model is a good fit for the data.

The revealed differences in the flotation response of slimes and medium-sized fractions of sphalerite activated by copper sulphate correlate with the results of bubble-particle attachment tests. As can be seen from Figure 11a,b increasing the rate of bubble-particle attachment (k) resulted in the growth of flotation recovery and flotation rate of sphalerite. Specifically, increasing the k from 0.0021 s^{-1} to 0.0249 s^{-1} increased ε from 28% to 82% and k_f from 0.093 min^{-1} to 0.273 min^{-1}. Moreover, increasing the rate of bubble-particle attachment increased the surface coverage of the bubble and hence resulted in the flotation recovery growth (see Figure 11c,d). The fitting equations for the dependencies between the ε and k, k_f and k, S and k, ε and S show high agreement with experimental data since the coefficient of determination (R^2) was in the range of 0.96–1. The strong correlation between the rate of bubble-particle attachment, the surface coverage of the bubbles with mineral particles, flotation recovery and rate indicates that k and S can be used as additional tools when choosing reagents in flotation.

Finally, we investigated the effect of water salinity on the flotation recovery of sphalerite under conditions of its depression with zinc sulphate and sodium sulphide at pH 9 and 10. The concentration of collectors and depressants were 0.01% and 0.1%, respectively. A strong depression of sphalerite flotation was observed with the combined action of zinc sulphate and sodium sulphide for both PIPX and SIDTP, indicating the extremely low flotation recovery of 1–6% and the lowest flotation rate of 0.02–0.003 min^{-1}. The effect of the salinity of sea water solutions, the type of collector and pH on the flotation recovery of sphalerite was insignificant. The flotation results correlate with bubble-particle attachment kinetics data. Specifically, we observed the lowest surface coverage of the bubbles (S = 0.5%) and attachment rates ($k = 3.3 \times 10^{-4} - 2.7 \times 10^{-5}$ s^{-1}) at conditioning time ranged from 15 s to 180 s, meaning insufficient bubble-particles attachment rates of depressed sphalerite particles result in extremely low surface coverage of the bubbles dropping down the sphalerite flotation recovery.

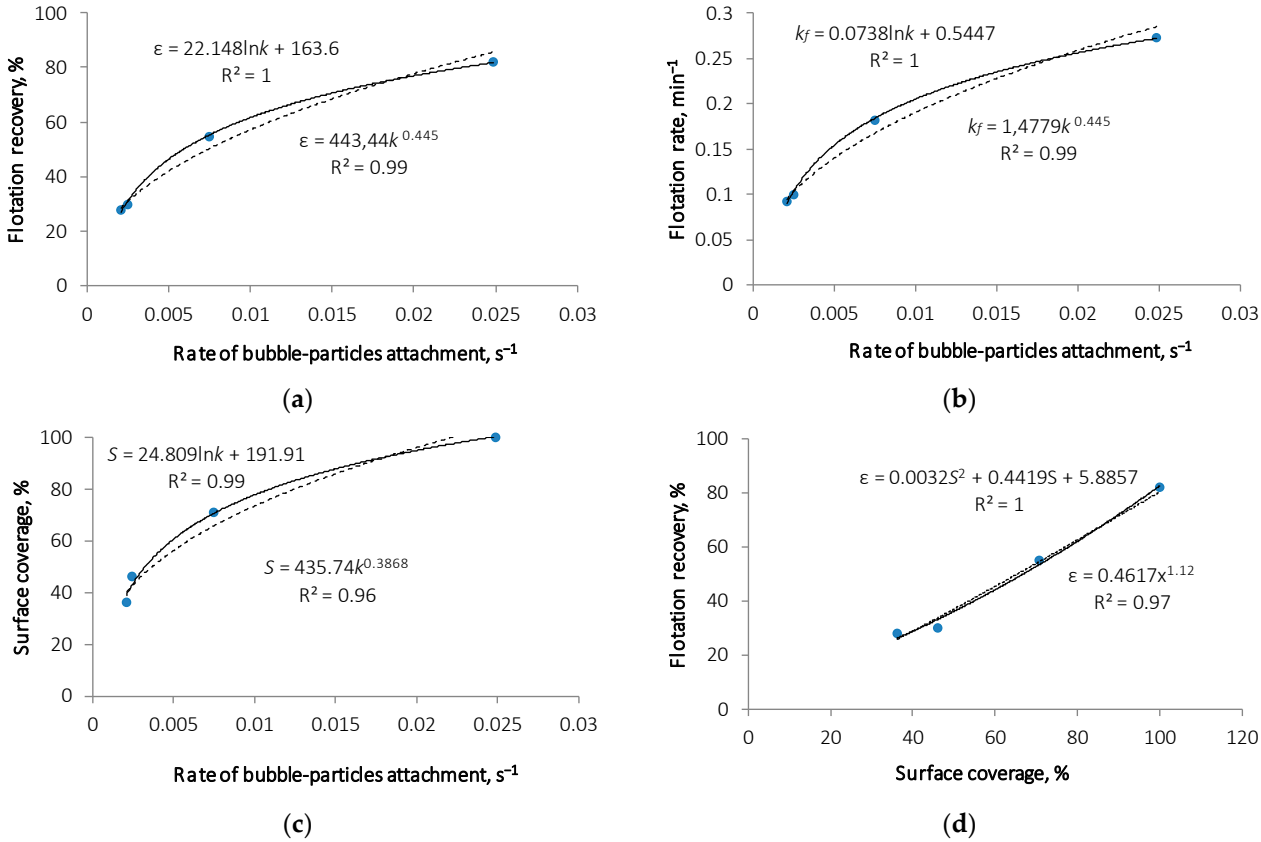

Figure 11. Fitting data for the effect of the rate of bubble-particles attachment on the flotation recovery (**a**), flotation rate (**b**), and surface coverage (**c**), and the effect of surface coverage on flotation recovery (**d**) using PIPX at water salinity of 2 g/L.

4. Conclusions

The findings showed the feasibility of sphalerite flotation in artificial sea water using conventional reagents (collectors, activators, and depressants). The correlations between the rate of bubble-particle attachment and the sphalerite flotation recovery were established, resulting in the growth of flotation recovery with the increase of the bubble-particle attachment rate. The results can be used as guidelines in choosing flotation reagents for sphalerite flotation in sea water. Another practical application of the results is the potential for sustainable development of the industrial sector, ecosystems and societies due to the replacement of fresh water by sea water, although further technological and environmental studies are required.

The study showed a linear trend for the bubble-particle attachment kinetics of non-activated sphalerite fractions of −74 + 44 μm and −44 μm in sea water solutions of PIPX and SIDTP. The copper sulphate increased the surface coverage of the bubbles with −74 + 44 μm sphalerite, whereas we observed a lower effect of activator on the slimes. The bubble-particle attachment kinetics of activated sphalerite slimes showed linearity. Moreover, the linear trend was observed for −74 + 44 μm sphalerite at low concentrations of copper sulphate; however, at its high concentrations, the first-order kinetic model for bubble-particle attachment was best described the experimental data. The effect of copper sulphate concentration on sphalerite flotation recovery in sea water was greater for a medium-sized fraction than for the slimes. PIPX performed better than SIDTP with respect to flotation of −74 + 44 μm activated sphalerite.

Regardless of salinity and collector type, the combined action of zinc sulphate and sodium sulphide in sea water solutions resulted in the lowest rate of bubble-particles attachment, flotation recovery and rate, meaning zinc sulphate and sodium sulphide can be used as depressants of sphalerite flotation in sea water.

Overall, the findings indicate that small-scale techniques can be used as a preliminary stage in choosing flotation reagents and modes for the flotation of base metals ores in sea water, saving resources and reducing environmental impact.

Future studies should be aimed at sea water flotation of large samples of sphalerite and fundamental research to understand the mechanisms of interaction of sphalerite and other target minerals with flotation reagents. Moreover, prospective research using flotation cells to test reagent modes to recover sphalerite using sea water and freshwater would be of practical interest.

Funding: This research received no external funding.

Data Availability Statement: Not applicable.

Conflicts of Interest: The author declares no conflict of interest.

References

1. Farjana, S.H.; Huda, N.; Parvez Mahmud, M.A.; Saidur, R. A review on the impact of mining and mineral processing industries through life cycle assessment. *J. Clean. Prod.* **2019**, *231*, 1200–1217. [CrossRef]
2. Seki, H.A.; Thorn, J.P.R.; Platts, P.J.; Shirima, D.D.; Marchant, R.A.; Abeid, Y.; Baker, N.; Annandale, M.; Marshall, A.R. Indirect impacts of commercial gold mining on adjacent ecosystems. *Biol. Conserv.* **2022**, *275*, 109782. [CrossRef]
3. Boldy, R.; Santini, T.; Annandale, M.; Erskine, P.D.; Sonter, L.J. Understanding the impacts of mining on ecosystem services through a systematic review. *Extr. Ind. Soc.* **2021**, *8*, 457–466. [CrossRef]
4. Nkuna, R.; Ijoma, G.N.; Matambo, T.S.; Chimwani, N. Accessing Metals from Low-Grade Ores and the Environmental Impact Considerations: A Review of the Perspectives of Conventional versus Bioleaching Strategies. *Minerals* **2022**, *12*, 506. [CrossRef]
5. Endl, A.; Gottenhuber, S.L.; Gugerell, K. Bridging Policy Streams of Minerals and Land Use Planning: A Conceptualisation and Comparative Analysis of Instruments for Policy Integration in 11 European Member States. In Proceedings of the REAL CORP 2020—SHAPING URBAN CHANGE, Aachen, Germany, 15–18 September 2020; pp. 95–105.
6. Abramov, A.A. *Tekhnologiya Obogashcheniya Rud Tsvetnykh Metallov*; Nedra: Moscow, Russia, 1983; p. 359.
7. Bulatovic, S.M. *Handbook of Flotation Reagents: Chemistry, Theory and Practice Flotation of Sulfide Ores*, 1st ed.; Elsevier: Amsterdam, The Netherlands, 2007; p. 727.
8. Herrera-Urbina, R.; Hanson, J.S.; Harris, G.H.; Fuerstenau, D.W. Principles and practice of sulphide mineral flotation. In *Sulphide Deposits—Their Origin and Processing*; Springer: Dordrecht, The Netherlands, 1990; pp. 87–101.
9. Castro, S.; Laskowski, J.S. Froth flotation in saline water. *KONA Powder Part. J.* **2011**, *29*, 4–15. [CrossRef]
10. Schneider, S.H.; Root, T.L.; Mastrandrea, M.D. *Encyclopedia of Climate and Weather*; Oxford University Press: New York, NY, USA, 1996; p. 1488.
11. Laskowski, J.S.; Castro, S.; Gutierrez, L. Flotation in seawater. *Mining, Metall. Explor.* **2019**, *36*, 89–98. [CrossRef]
12. Cisternas, L.A.; Gálvez, E.D. The use of seawater in mining. *Miner. Process Extr. Metall. Rev.* **2018**, *39*, 18–33. [CrossRef]
13. Moreno, P.A.; Aral, H.; Cuevas, J.; Monardes, A.; Adaro, M.; Norgate, T.; Bruckard, W. The use of seawater as process water at Las Luces copper-molybdenum beneficiation plant in Taltal (Chile). *Miner. Eng.* **2011**, *24*, 852–858. [CrossRef]
14. Levay, G.; Smart, R.S.C.; Skinner, W.M. The impact of water quality on flotation performance. *J. S. Afr. Instig. Min. Metall.* **2001**, *101*, 69–75.
15. Liu, W.; Moran, C.J.; Vink, S. A review of the effect of water quality on flotation. *Miner. Eng.* **2013**, *53*, 91–100. [CrossRef]
16. Wang, B.; Peng, Y. The effect of saline water on mineral flotation—A critical review. *Miner. Eng.* **2014**, *66–68*, 13–24. [CrossRef]
17. Meißner, S. The Impact of Metal Mining on Global Water Stress and Regional Carrying Capacities—A GIS-Based Water Impact Assessment. *Resources* **2021**, *10*, 120. [CrossRef]
18. Carvalho, J.; Galos, K.; Kot-Niewiadomska, A.; Gugerell, K.; Raaness, A.; Lisboa, V. A look at European practices for identifying mineral resources that deserve to be safeguarded in land-use planning. *Resour. Policy* **2021**, *74*, 102248. [CrossRef]
19. Suopajärvi, L.; Beland Lindahl, K.; Eerola, T.; Poelzer, G. Social aspects of business risk in the mineral industry—Political, reputational, and local acceptability risks facing mineral exploration and mining. *Miner. Econ.* **2022**. [CrossRef]
20. Ihle, C.F.; Kracht, W. The relevance of water recirculation in large scale mineral processing plants with a remote water supply. *J. Clean. Prod.* **2018**, *177*, 34–51. [CrossRef]
21. Suyantara, G.P.W.; Hirajima, T.; Miki, H.; Sasaki, K. Floatability of molybdenite and chalcopyrite in artificial seawater. *Miner. Eng.* **2018**, *115*, 117–130. [CrossRef]
22. Li, Y.; Zhu, H.; Li, W.; Zhu, Y. A fundamental study of chalcopyrite flotation in sea water using sodium silicate. *Miner. Eng.* **2019**, *139*, 105862. [CrossRef]
23. Ramirez, A.; Rojas, A.; Gutierrez, L.; Laskowski, J.S. Sodium hexametaphosphate and sodium silicate as dispersants to reduce the negative effect of kaolinite on the flotation of chalcopyrite in seawater. *Miner. Eng.* **2018**, *125*, 10–14. [CrossRef]
24. Hirajima, T.; Suyantara, G.P.W.; Ichikawa, O.; Elmahdy, A.M.; Miki, H.; Sasaki, K. Effect of Mg^{2+} and Ca^{2+} as divalent seawater cations on the floatability of molybdenite and chalcopyrite. *Miner. Eng.* **2016**, *96–97*, 83–93. [CrossRef]

25. Peng, Y.; Seaman, D. The flotation of slime-fine fractions of Mt. Keith pentlandite ore in de-ionised and saline water. *Miner. Eng.* **2011**, *24*, 479–481. [CrossRef]
26. Castellón, C.I.; Piceros, E.C.; Toro, N.; Robles, P.; López-Valdivieso, A.; Jeldres, R.I. Depression of pyrite in seawater flotation by guar gum. *Metals* **2020**, *10*, 239. [CrossRef]
27. Zhong, H.; Huang, Z.X.; Zhao, G.; Wang, S.; Liu, G.; Cao, Z. The collecting performance and interaction mechanism of sodium diisobutyl dithiophosphinate in sulfide minerals flotation. *J. Mater. Res. Technol.* **2015**, *4*, 151–161. [CrossRef]
28. Chandra, A.P.; Gerson, A.R. A review of the fundamental studies of the copper activation mechanisms for selective flotation of the sulfide minerals, sphalerite and pyrite. *Adv. Colloid Interface Sci.* **2009**, *145*, 97–110. [CrossRef]
29. Uddin, S.; Li, Y.; Mirnezami, M.; Finch, J.A. Effect of particles on the electrical charge of gas bubbles in flotation. *Miner. Eng.* **2012**, *36–38*, 160–167. [CrossRef]
30. Chu, P.; Mirnezami, M.; Finch, J.A. Quantifying particle pick up at a pendant bubble: A study of non-hydrophobic particle-bubble interaction. *Miner. Eng.* **2014**, *55*, 162–164. [CrossRef]
31. Nikolaev, A.A.; Konyrova, A.; Goryachev, B.E. A study on the mineralization kinetics of an air bubble in a suspension of activated and non-activated sphalerite. *Obogashchenie Rud.* **2020**, *1*, 26–31. [CrossRef]
32. Nikolaev, A.A. Flotation recovery of toner containing iron oxide from water suspension. *Miner. Eng.* **2019**, *144*, 106027. [CrossRef]
33. Nikolaev, A.A.; Batkhuyag, A.; Goryachev, B.E. Mineralization kinetics of air bubble in pyrite slurry under dynamic conditions. *J. Min. Sci.* **2018**, *54*, 840–844. [CrossRef]
34. Nikolaev, A.A.; Soe, T.; Goryachev, B.E. Criterion of collector's selectivity in sulfide ores bulk-selective flotation circuits. *Obogashchenie Rud.* **2016**, *4*, 23–28. [CrossRef]
35. Nikolaev, A.A.; Petrova, A.A.; Goryachev, B.E. Pyrite grain and air bubble attachment kinetics in agitated pulp. *J. Min. Sci.* **2016**, *52*, 352–359. [CrossRef]
36. Nikolaev, A.A.; Soe, T.; Goryachev, B.E. Upon bubble-mineral attachment kinetics with sphalerite under the conditions of application of thiol collectors and mixtures of these collectors. *Obogashchenie Rud.* **2016**, *5*, 14–18. [CrossRef]
37. Song, S.; Lopez-Valdivieso, A.; Reyes-Bahena, J.L.; Lara-Valenzuela, C. Floc flotation of galena and sphalerite fines. *Miner. Eng.* **2001**, *14*, 87–98. [CrossRef]
38. Boulton, A.; Fornasiero, D.; Ralston, J. Characterisation of sphalerite and pyrite flotation samples by XPS and ToF-SIMS. *Int. J. Miner. Process* **2003**, *70*, 205–219. [CrossRef]
39. Wang, P.; Reyes, F.; Cilliers, J.J.; Brito-Parada, P.R. Evaluation of collector performance at the bubble-particle scale. *Min. Eng.* **2020**, *147*, 106140. [CrossRef]
40. Rao, F.; Lázaro, I.; Ibarra, L.A. Solution chemistry of sulphide mineral flotation in recycled water and sea water: A review. *T. I. Min. Metall. C* **2017**, *126*, 139–145. [CrossRef]
41. Houot, R.; Raveneau, P. Activation of sphalerite flotation in the presence of lead ions. *Int. J. Miner. Process* **1992**, *35*, 253–271. [CrossRef]
42. Klassen, V.I.; Mokrousov, V.A. *An Introduction to the Theory of Flotation*; Butterworths: London, UK, 1963.
43. Jeldres, R.I.; Forbes, L.; Cisternas, L.A. Effect of Seawater on Sulfide Ore Flotation: A Review. *Min. Proc. Ext. Met. Rev.* **2016**, *37*, 369–384. [CrossRef]
44. Peng, Y.; Bradshaw, D. Mechanisms for the improved flotation of ultrafine pentlandite and its separation from lizardite in saline water. *Miner. Eng.* **2012**, *36–38*, 284–290. [CrossRef]
45. Nikolaev, A.A.; Konyrova, A.; Goryachev, B.E. Wetting of sphalerite, chalcopyrite and pyrite in treatment with sulfhydryl collectors in saltish and sea water. *J. Min. Sci.* **2020**, *56*, 654–662. [CrossRef]
46. Wang, J.; Xie, L.; Liu, Q.; Zeng, H. Effects of salinity on xanthate adsorption on sphalerite and bubble–sphalerite interactions. *Miner. Eng.* **2015**, *77*, 34–41. [CrossRef]